EXPERIMENTAL AND NUMERICAL MODELLING OF FLOWS IN FISH SHELTERS DOWNSTREAM OF HYDROELECTRIC PLANTS

Vera Almeida

ABSTRACT

Hydroelectric power production introduces alterations in the watercourses downstream of powerplants due to the magnitude and frequency of the turbinated flows. This phenomenon is called hydropeaking and leads to changes in the natural flow regime as well as in the downstream existing ecosystems, causing severe adversities to the well-being of the fish population.

The main purpose of this dissertation is acquiring better knowledge regarding the geometry of fish shelters downstream of hydroelectric plants. A 3D model was developed based on an experimental installation in the Laboratory of Hydraulic Structures and Environment at Instituto Superior Técnico. A set of deflectors were installed in a rectangular section flume to simulate lateral fish shelters. To characterize different peak flows, three scenarios were simulated: 7, 22 and 50 l/s. Flow depths were measured and an acoustic Doppler velocimeter (ADV) was used to obtain the velocities in the flume. A numerical study of the 3D model was developed using FLOW 3D®, a computational fluid dynamics (CFD) software. The results of velocity and turbulent kinetic energy (TKE) obtained numerically and experimentally were compared. After the model was calibrated and validated, alternative shelter configurations were developed and the respective flow was characterized considering the previous parameters.

Numerical and experimental results for the velocity fields were concordant. The model presented some limitations reproducing TKE values obtained experimentally. Using FLOW 3D to characterize the flow for the alternative geometries allowed to save time and resources, which would be required in experimental trials.

Key-words: Hydropeaking, fish shelters, experimental installation, acoustic Doppler velocimeter (ADV), computational fluid dynamics (CFD), FLOW-3D®

1. INTRODUCTION

During peak operations, hydroelectric powerplants rapidly increase or decrease the discharge to the river, causing rapid changes in water depth and velocity downstream. This phenomenon is called hydropeaking and has currently been raising more concerns each day because of the role renewable energy production is achieving in power production worldwide.

Hydropeaking is considered as an anthropogenic flow alteration downstream of hydropower plants with severe effects on freshwater ecosystems (Charmasson & Zinke, 2011). Alterations to the natural behaviour of flow in watercourses can be divided in hydraulic, morphologic or water quality related (Meile, 2006). These alterations stem into biotic impacts, particularly on the existing fish populations, leading to losses in habitat availability and a decline in the number of individuals (Scruton et al. 2008; Person 2013; Boavida et al. 2015). Fish are commonly used to study hydropower operations impacts on the rivers, since these populations are considered a good indicators of the environmental state of the ecosystem (Young, Cech e Thompson, 2011).

Mitigation measures of hydropeaking can be divided into three groups: operational, structural and morphologic (Person, 2013). Operational measures are related to the hydropower plants operations management (Clarke et al. 2008; Charmasson & Zinke 2011). Structural and morphological measures consist of physical modifications related to the construction of structures in the watercourses or morphological restoration of the river bed aiming to reduce the impacts of hydropeaking (Ribi et al. 2010).

Biotic impacts such as fish stranding or drifting, increase of stress and fatigue and reduction in reproduction activity are common for fish in hydropeaking rivers (Person, 2013). Fish shelters are

highlighted as a possible physical mitigation measure to be implemented downstream of hydropower plants regarding the biotic hydropeaking impacts seen on fish populations (Ribi et al. 2010; Almeida et al. 2014). However, this type of mitigation is a subject to be given a greater focus in future works, since it is still poorly explored (Ribi et al., 2014).

The interaction between the physical properties of the flow (e.g. water depth, velocity, shear stress or turbulence) and biologic responses of the aquatic organisms to alterations of the natural state of a river is a complex subject due to the great possibility of cause-effect associations. Harby & Noack (2013) present three possible approaches to study hydropeaking and evaluate the efficiency of different mitigation measures: laboratory experiments, experimental in-situ studies and numerical modelling.

Laboratory trials allow the understanding of isolated rapid flow fluctuations effects. However, it can be challenging to reproduce in laboratory the morphologic conditions of river, as well as realistic flow coefficients and rates. In-situ trials have a great variability of characteristics associated to each experiment, making comparisons to reference cases problematic. These two types of approach can be demanding and take a considerable amount of time, not to mention the inaccessibility to certain areas of the watercourses.

The use of numerical models (computational fluid dynamics -CFD) as a mean to increase the existing understanding concerning hydropeaking structural mitigation has great utility. These models, if properly calibrated and validated ease the analysis of hydraulic parameters for a set of different scenarios. By dismissing the physical reproduction of diverse configuration or scenarios options, these models become a strong tool supporting the development of new solutions. The conjugation between experimental trials and numerical simulations has become the most viable option to test the efficiency of structural mitigation measures (Harby & Noack, 2013). The increasing use of hydroelectric energy leads to the need of developing studies which can support an adequate selection of efficient mitigation strategies.

The main objective of this study is to acquire better knowledge regarding the geometry of fish shelters downstream of hydroelectric plants. Firstly, experimental trials were carried out in an experimental indoor flume equipped with lateral refuges. The flow was characterized in terms of velocity, water depth and turbulent kinetic energy (TKE). These results were used to calibrate and validate a 3D numerical model of the flume, developed with the commercial software FLOW-3D®. Three alternative geometries for the shelters were developed and analysed in terms of their hydraulic parameters.

2. MATERIALS AND METHODS

2.1. Flume Experimental Setup

The experiments, in the present study, were carried out in an indoor flume at the Laboratory of Hydraulic Structures and Environment at Instituto Superior Técnico, Lisbon, Portugal. The flume consists in a rectangular section channel with 8,00 m length, 0,70 m width and 0,70 m high. The channel is supplied by a reservoir. Both inlet and outlet of the channel are controlled by adjustable gates (Figure 1).

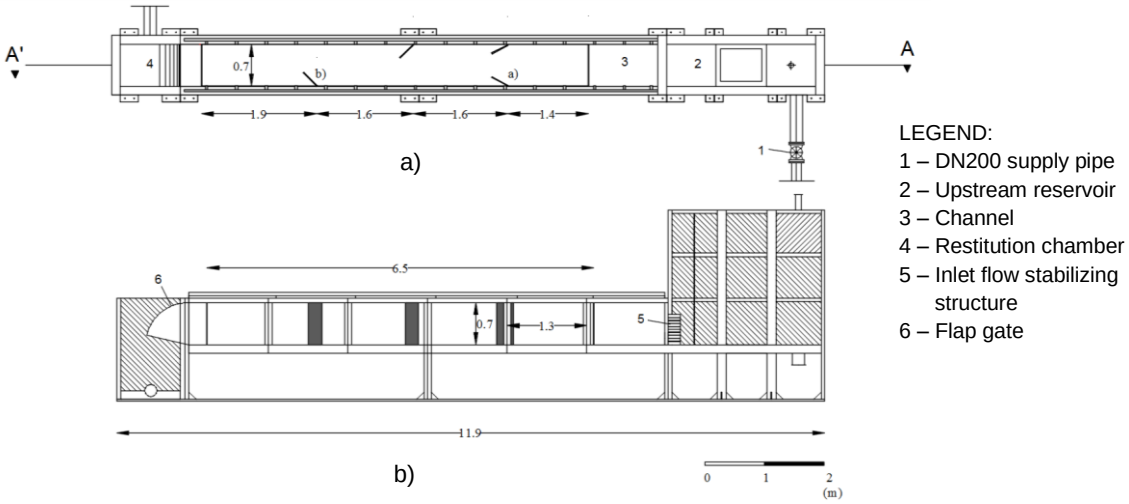

Figure 1 – Experimental setup - (a) Top and (b) lateral view of the flume.

A set of 4 deflectors (0,30 x 0,76 m and 0,015 m width) were installed in the channel to simulate fish shelters. The deflectors were positioned with different opening angles to create heterogenous flow conditions. Figure 2 presents geometric details of both deflectors. A total channel length of 6,5 m was characterized during the trials. This length corresponds to the distance between two perforated metal sheets, installed on upstream and downstream sections of the channel. Table 1 synthetizes the dimensions of each one of the installation elements.

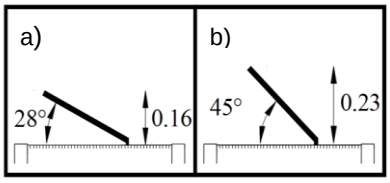

Figure 2 – Deflectors a) and b) details

Table 1 -Summary of the dimensions of the experimental installation elements

		Dimensions
Channel	Length (m)	6,50
	Width (m)	0,70
Deflectors (4)	Length (m)	0,76
	Width (m)	0,30
	Thickness (cm)	1,50
Upstream Gate	Opening Angle (º)	10,0
Downstream Gate	Opening Angle (º)	72,0

Three hydropeaking scenarios were simulated: 7 l/s, 22 l/s and 50 l/s. These correspond respectively to a base flow, and two peak flow scenarios. The defined measuring grid mesh consisted of 103 points with a minimum spacing of 10 cm next to the deflectors and between 15 to 52 cm in the remaining sections of the channel. This mesh allows a better characterization of the hydraulic conditions near the deflectors, having into account the purpose of the present work. The measures were undertaken at a 5 cm depth. Velocities were measured on these points through an Acoustic Doppler Velocimeter (ADV) with a frequency of 100 Hz during a sampling period of 180 s, which is considered to be adequate for accurate velocity measurements (Quaresma et al., 2017). Due to the oscillations of the free surface, water depth intervals were measured at the upstream and downstream sections of the channel. Velocity magnitude and turbulent kinetic energy were, respectively, obtained from the expressions (1) $V = \sqrt{\bar{u}^2 + \bar{v}^2 + \bar{w}^2}$ and (2) $k = \frac{1}{2}(\overline{u'^2} + \overline{v'^2} + \overline{w'^2})$, where u corresponds to the longitudinal, v the transverse and w the vertical velocity directions. These parameters were used to calibrate and validate the 3D model of the channel developed in FLOW-3D®.

2.2. Numerical Model

2.2.1. FLOW-3D®

The chosen software for the present study was FLOW-3D®, which is a commercial CFD code, developed by FlowScience, Inc. This software presents a wide range of modelling capabilities of free surface fluid flow with great precision. One of the approaches FLOW-3D®uses to simulate turbulent flows is Reynolds averaging (time averaging the Navier-Stokes equations) yielding the so-called Reynolds averaged Navier-Stokes (RANS) equations. One of the RANS turbulence models that FLOW-3D® has available is the RNG k – ε turbulence model. The above turbulence model consists of two transport equations, one for the turbulent kinetic energy, k, and the other for the turbulent dissipation rate, ε. FLOW-3D®uses the algorithm TruVOF™ to accurately predict free-surface flows, which neglects the effect of the air above the surface (and its contact zone with the fluid in the simulation), treating it as a region without fluid mass (void) with a standard pressure assigned to it. FAVOR™ method (acronym for Fractional Area/Volume Obstacle Representation), used exclusively by FLOW-3D® is used to define general geometric regions within the rectangular grid, allowing to represent complex geometries at a level consistent with the use of average flow quantities within each volume element (Flow Science, 2018).

2.2.2. Numerical Model Implementation

A 3D model of the experimental flume was created in *AutoCAD* and imported to FLOW-3D®. A uniform cubic mesh with 2 cm edges was applied to the channel domain – Figure 3a). After rendering the geometry through FAVOR ™ method, it was concluded that a finest mesh was needed, since the deflectors were not being correctly reproduced. Three nested blocks of 1.0 cm edges cubic cells were applied in the deflectors regions – Figure 3b) - allowing greater detail in the definition of the deflectors geometry as well as greater precision in the calculations of the respective volume.

The upstream (Y_{min}) and downstream (Y_{max}) boundaries of the coarse mesh block were defined as specified pressure conditions with the definition of the fluid elevation measured experimentally. Wall boundary conditions were defined in the following plans: Z_{min}, X_{min} and X_{max}, representing the bottom and the walls of the channel, respectively. Above the free surface, it was considered a Specified Pressure condition to Z_{max}. and the atmospheric pressure was considered. Regarding the fine mesh blocks, symmetry conditions were considered to ensure that the flow conditions are maintained in the transition between the coarse and the fine mesh block. The top, bottom and lateral boundaries of fine mesh blocks are coincident with the coarse mesh block boundaries. As a final condition it was guaranteed that for every simulation the steady state was reached.

The activated physical models were: Gravity and non-inertial reference frame and Viscosity and turbulence. The chosen turbulence model was RNG κ-ε. The Maximum Turbulent Length Scale (TLEN) was set to be dynamically computed by FLOW-3D®. These options have already been used and validated by other authors through sensitivity analysis and comparison between experimental and numerical results (Silva, 2013; Lúcio, 2015; Pereira, 2016; Nunes, 2017). Regarding the numerical approximation of advection terms, a second order scheme with monotonicity preserving was defined in the simulations. FLOW-3D®. Silva (2013) assessed the effects of considering this method in the simulations, concluding that by a small increase of the simulation time, a good correlation between numerical and experimental results was found.

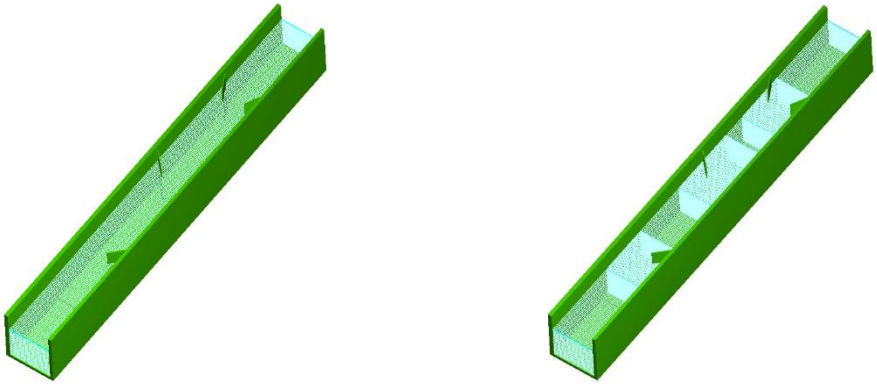

(a) (b)

Figure 3 - (a) Uniform coarse mesh block and (b) Introduction of nested blocks in relevant hydraulic zones

Two porous baffles were inserted at the upstream and downstream boundaries of the channel. The implementation of these pretended to solve the lack of stability of the hydraulic parameters during the simulation – Figure 4, noting that the steady state was not reached. The baffles are flux surfaces and their definition in FLOW-3D® consists on the definition of four parameters: position, geometry, porosity and head loss coefficients. The porosity was defined as 0,41. This value corresponds to the porosity of the existing perforated metal sheets in the experimental installation. To ensure a correct characterization of these elements, it was found that the linear head loss coefficient (KBAF1) should be properly defined. KBAF1 was obtained through the relation between the head loss due to a singularity and the head loss due to an enlargement. After the correct definition of all these parameters, it was possible to reach the steady-state – Figure 5.

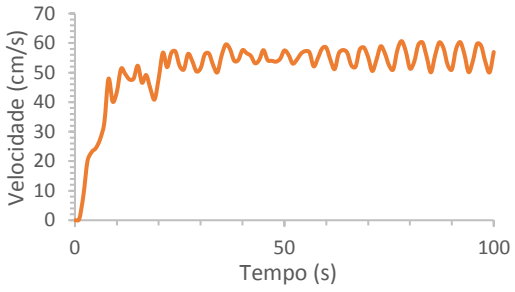

Figure 4 – Velocity-Time graph for the coordinate (x,y,z) = (0,35; 3,2; 0,05) m without baffles

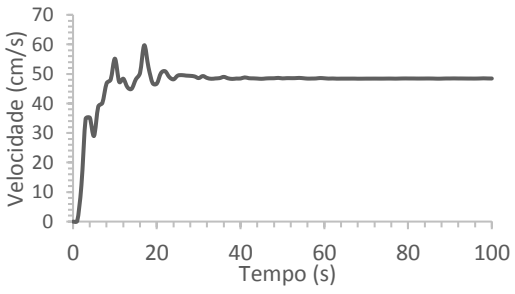

Figure 5 - Velocity-Time graph for the coordinate (x,y,z) = (0,35; 3,2; 0,05) m with baffles

A mesh independency analysis was carried out to understand the relation between the results and the cell dimensions. This analysis was performed for the 22 l/s scenario and considered a 50% reduction in both coarse and fine mesh cells dimensions. A summary of the meshes considered for the present study can be seen in Table 2. The comparison between the results obtained with both meshes was performed for flow, velocities and turbulent kinetic energy. As can be seen in Figure 6, both cases resulted in similar variations of flow during the simulation time. A percentage difference of less than 1% was calculated between the two obtained flows (Q_{mesh-1} = 21,95 l/s; Q_{mesh-2} = 21,86 l/s).
In terms of velocity, an average variation of 1,1 cm/s was calculated between the velocities obtained through mesh 1 and mesh 2- Maximum difference calculated was 7,2 cm/s. In terms of TKE an average difference of 2,9 cm^2/s^2 and a maximum difference of 19,5 cm^2/s^2 were observed.

Table 2 – Summary of the meshes used for the numerical model

Mesh	Nº of blocks	Cell Size (m)	No. of Cells
Mesh 1	1 coarse	2,0 cm	2563547
	3 refined	1,0 cm	
Mesh 2	1 coarse	1,0 cm	8614012
	3 refined	0,5 cm	

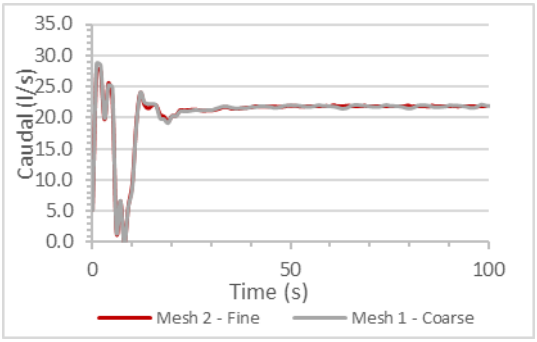

Figure 6 –Flowrate obtained for mesh 1 and mesh 2

2.2.1. Alternative Fish Shelters Geometries

Three alternative models were developed with the purpose of comparing the different velocity and TKE distributions in the flume originated by different fish shelter configurations. The 3D models were created in *AutoCAD* and then imported to FLOW-3D®. The methods and conclusions taken from the calibration phase were considered during the alternative configurations simulations. Also, all the three configurations were tested for the three defined scenarios (7, 22 and 50 l/s).
Geometry G0 consists of the channel without any type of obstacle – Figure 7. This geometry allows the comparison of the flow parameters between the presence and the absence of shelters. It can be a reference to future analysis, biologic or hydraulic.

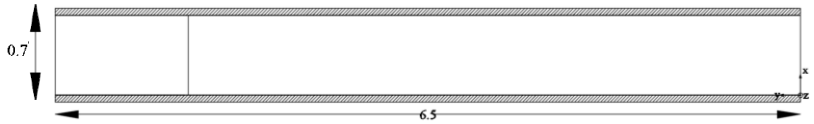

Figure 7 – Top view of geometry G0

Geometry G1 is similar to the geometry studied during the model calibration. However, it was developed with the purpose of creating a more homogeneous flow, since all the deflectors were installed in the same side of the channel – Figure 8. Furthermore, this configuration is closer to what can be a river intervention, since most of the times, only one side of the river is accessible. The deflectors were installed in the same transversal sections as the ones in the first geometry. All the deflectors are opened with the same angle (45º).

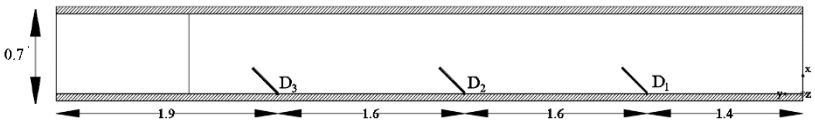

Figure 8 – Top view of geometry G1

Geometry G2 presents a new concept of shelter, when compared with the previous ones. For this configuration, three triangular open blocks were installed along the channel – Figure 9. These blocks were designed taking into account existing works concerning fish passages (Heimerl et al., 2008; Santos

et al., 2014). In these studies, the dimension of the blocks was defined in function of the morphology and the stage of life of the species tested on the experimental trials.

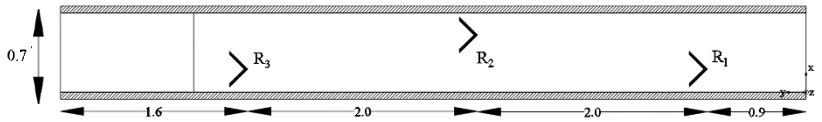

Figure 9 – Top view of geometry G2

3. RESULTS

3.1. Calibration

After the model was calibrated and validated, it was concluded that the numerical model consisted of a good approximation to the results obtained experimentally. The velocity in the channel – Figure 10 - varies between approximately 0 cm/s downstream of the deflectors and a maximum of 18,9 cm/s for 7 l/s, 42,7 cm/s for 22 l/s and 71,9 cm/s for the peak flow, 50 l/s. Maximum velocities occur near the deflectors, since these seem to create a wake in the flow, causing higher velocity values.

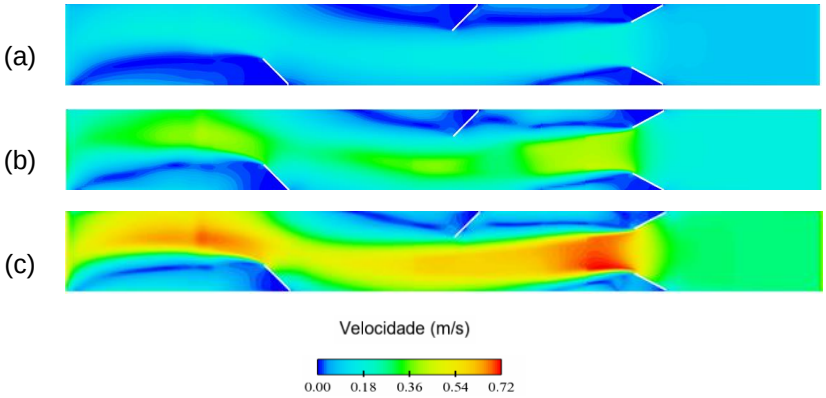

Figure 10 – Geometry Calib - Velocity distribution for (a) 7 l/s, (b) 22 l/s and (c) 50 l/s. Longitudinal profile z = 0,05 m.

The upstream sections of the flume correspond to zones with practically zero turbulence for all the three scenarios, as can be seen in Figure 11. The maximum TKE values occurred downstream of the deflectors and correspond to 12,8; 57,2 and 181,4 cm^2/s^2, for 7, 22 and 50 l/s, respectively.

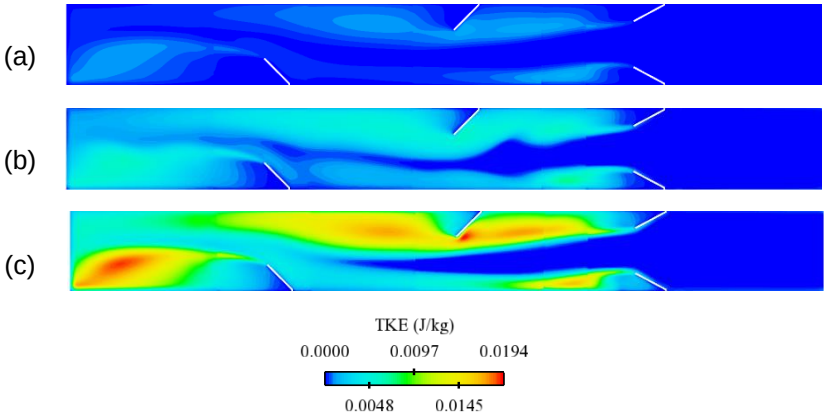

Figure 11 – Geometry Calib - TKE distribution for (a) 7 l/s, (b) 22 l/s and (c) 50 l/s. Longitudinal profile z = 0,05 m.

3.2. Alternative Geometries

Geometry G0

The lack of obstacles in the channel origins a uniform velocity distribution (Figure 12) in the flow domain, with average velocities being calculated as 10,0 cm/s, 21,5 cm/s and 38,1 cm/s for 7,22 and 50 l/s,

respectively. The standard-deviation was less or equal to 1,1 cm/s for the three simulated scenarios, confirming the expected flow uniformity.

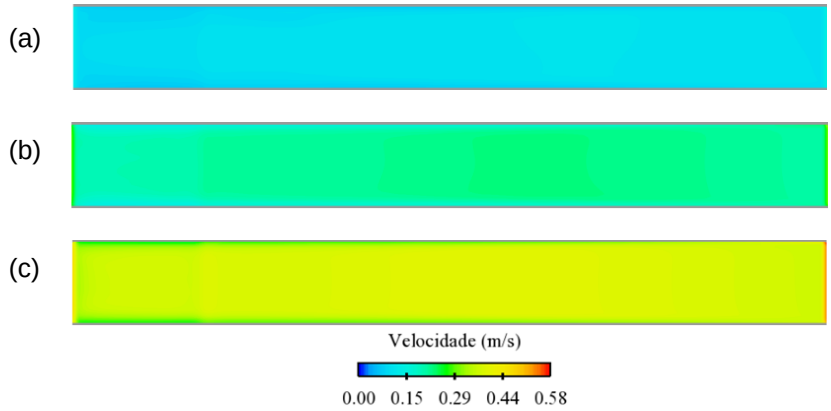

Figure 12 - Geometry G0 - Velocity distribution for (a) 7 l/s, (b) 22 l/s and (c) 50 l/s Longitudinal profile z = 0,05 m.

Figure 13 consists of the TKE distribution on the flow domain for the geometry G0, considering the three flow scenarios. TKE is approximately 0,0 cm^2/s^2 in the initial section of the channel. The TKE increases downstream for the three studied scenarios, reaching medium values of 0,3 cm^2/s^2 to 7 l/s, 0,9 cm^2/s^2 to 22 l/s and 1,0 cm^2/s^2 to 50 l/s.

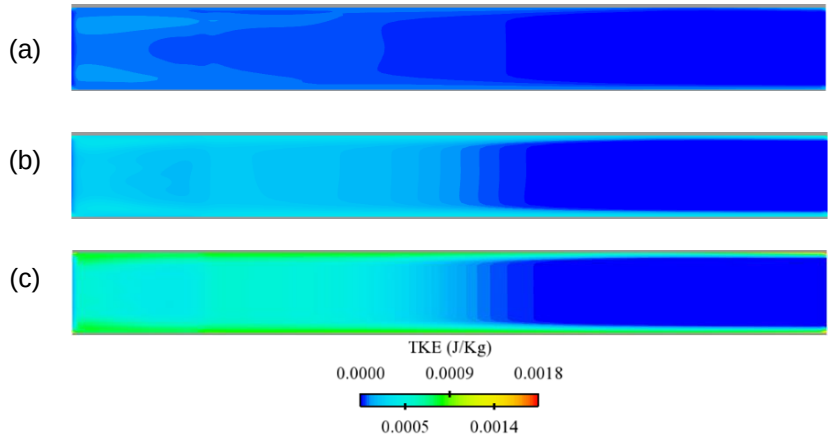

Figure 13 – Geometry G0 – TKE distribution for (a) 7 l/s, (b) 22 l/s and (c) 50 l/s. Longitudinal profile z = 0,05 m.

Geometry G1

The velocities distribution for geometry G1 (Figure 14) is similar to the distribution observed with the calibration geometry. Downstream the shelters, velocities are close to 0 cm/s. Strong variations are seen at the transversal sections level, since within a limited space, velocity varies between 0 cm/s and a maximum value, occurring due the wake originated by the deflector. Although this velocity field has similarities with the first model developed, with standard deviations in the same order of magnitude (5.5, 12.3 and 19.7 cm/s for 7, 22 and 50 l/s respectively), the observed velocity distribution over the flume domain for geometry G1 can be divided into two zones: one, on the deflectors side of the channel where velocities have reduced values; and other where velocities reach higher values. Average velocities achieved with this geometry are 9,4 cm/s for the 7 l/s scenario, 20,6 cm/s for the 22 l/s scenario and 33,4 cm/s for the peak flow 50 l/s. As can be seen in Table 3, these values are very close to the ones obtained with the calibration geometry.

When analysing Figure 15, regarding TKE distribution on the channel considering geometry G1, the high turbulence downstream of the deflectors caused by the presence of these can be highlighted. On the other side of the channel, low TKE values are common for the three scenarios. Average values of TKE were computef as 1,9; 11,3 and 42.8 cm^2/s^2 for 7,22 and 50 l/s flows, respectively. Regarding the variation of TKE within the respective channel domain, standard-deviation was computed as 2,9; 16,1

and 54,7 cm^2/s^2 for 7,22 and 50 l/s flows, respectively. Once again these values are very close to the ones obtained with the first configuration modelled (geometry G-calib).

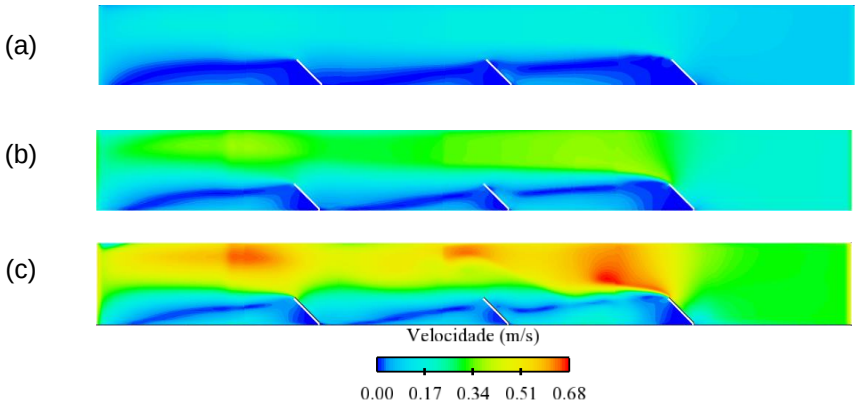

Figure 14 - Geometry G1 - Velocity distribution for (a) 7 l/s, (b) 22 l/s and (c) 50 l/s. Longitudinal profile z = 0,05 m.

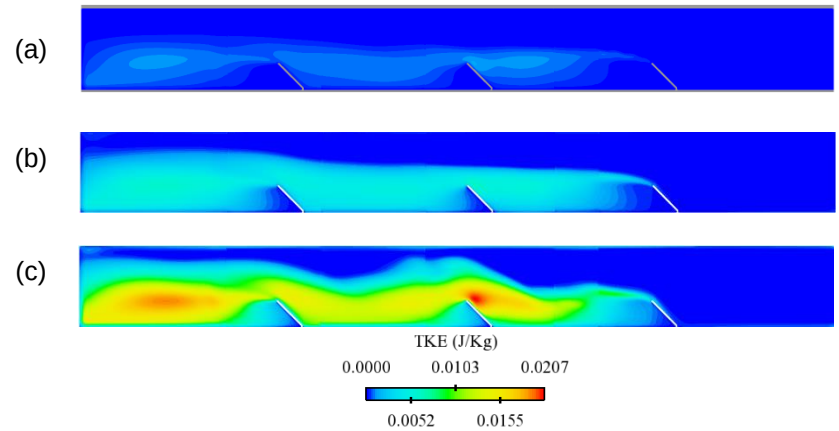

Figure 15 - Geometry G1 - TKE distribution for (a) 7 l/s, (b) 22 l/s and (c) 50 l/s Longitudinal profile z = 0,05 m.

Geometry G2

This configuration provides a greater dispersion of the hydraulic parameters within the flow domain. The abrupt variation of these parameters within a small influence area downstream the triangular obstacles can be highlighted. Average velocities for this configuration were calculated as 7,9; 17,8 and 30,3 cm/s and the correspondent standard deviation calculated as 4,1; 6,8 and 11,5 cm/s for the 7, 22 and 50 l/s, respectively.

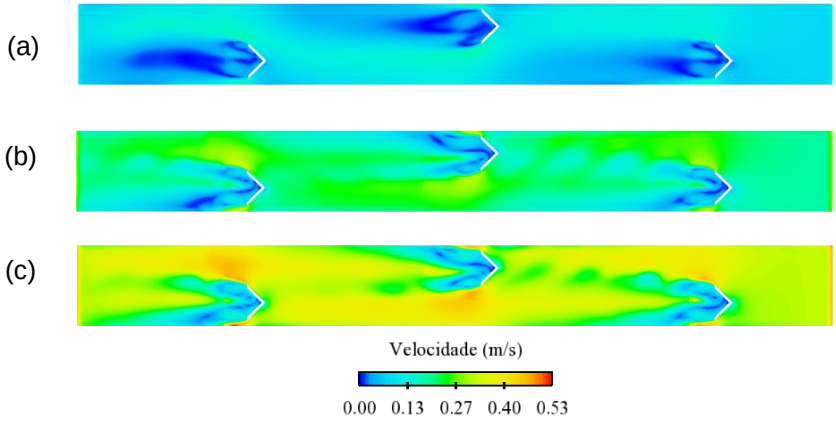

Figure 16 - Geometry G2 - Velocity distribution for (a) 7 l/s, (b) 22 l/s and (c) 50 l/s Longitudinal profile z = 0,05 m.

Average TKE was calculated as 4,0; 13,6 and 31,8 cm^2/s^2 to 7, 22 and 50 l/s flows, respectively. TKE standard-deviation was calculated as 4,9; 15,4 and 34,2 cm^2/s^2 to 7, 22 and 50 l/s respectively. This

shelter configuration is the one that confers a more heterogeneous velocity and TKE distribution downstream the shelters. However, quantitatively this is not reflected in the results, since this configuration has in general lower values of velocity and TKE standard-deviation, comparing to G1 and G-calib.

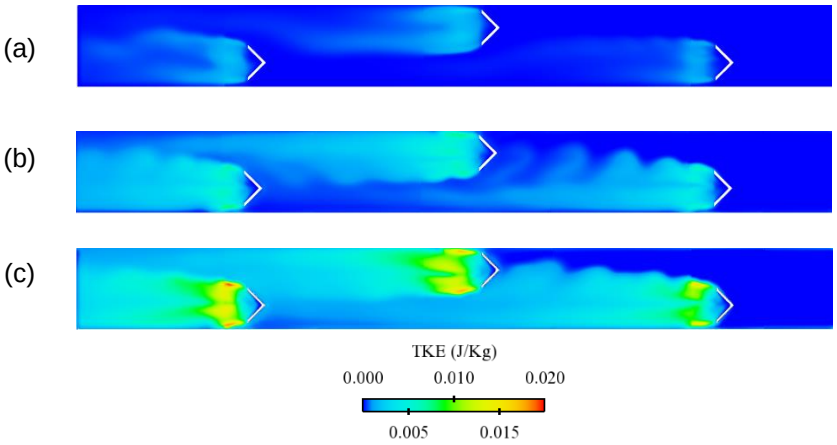

Figure 7 - Geometry G2 - TKE distribution for (a) 7 l/s, (b) 22 l/s and (c) 50 l/s. Longitudinal profile z = 0,05 m.

All the data discussed above is synthetized and presented in Table 3.

Table 3 -Summary of the flow parameters

	G0			G1			G2			G-calib		
Flow (l/s)	**7,0**	**22,0**	**50,0**	**7,0**	**22,0**	**50,0**	**7,0**	**22,0**	**50,0**	**7,0**	**22,0**	**50,0**
Max velocity (cm/s)	10,5	22,4	39,5	16,8	37,9	66,7	15,6	29,1	47,3	18,9	42,7	71,9
Min velocity (cm/s)	8,8	19,3	35,0	0,2	0,5	1,0	0,7	2,2	3,6	0,1	0,3	0,9
Ave velocity (cm/s)	10,0	21,5	38,1	9,4	20,4	33,2	7,9	17,8	30,3	9,2	20,2	34,5
Std Dev velocity (cm/s)	0,4	0,7	1,1	5,7	12,3	19,9	4,1	6,8	11,5	5,4	12,0	30,4
Max TKE (cm^2/s^2)	0,7	2,7	7,0	10,8	56,4	201,1	23,1	64,1	138,6	12,8	57,2	181,4
Min TKE (cm^2/s^2)	0,0	0,0	0,0	0,0	0,0	0,0	0,0	0,0	0,0	0,0	0,0	0,0
Ave TKE (cm^2/s^2)	0,3	0,9	2,0	1,9	10,5	40,1	4,0	13,6	31,8	3,0	15,3	44,7
Std Dev TKE (cm^2/s^2)	0,2	0,9	2,3	2,9	15,3	53,4	4,9	15,4	34,2	3,5	17,1	51,1

4. Conclusions

The presented work consisted of the development of a 3D CFD model, calibrated and validated based on experimental trials results carried out in an indoor artificial flume where fish shelters were installed.
The numerical model developed with the software FLOW-3D® provided velocity and TKE distribution over the flume domain for three scenarios: 7, 22 and 50 l/s. In a general way, it is considered that this software was able to accurately reproduce the flow behaviour in the presence of the fish shelters. Velocities obtained with the numerical model are very close to the ones obtained during the carried out experimental trials, being this a common conclusion for all the three analysed scenarios. Determination coefficients, R^2, were calculated as 0,878; 0,882 and 0,872 for 7, 22 and 50 l/s, respectively. These results reflect how well the CFD model reproduces values obtained experimentally.
Regarding TKE values, obtained numerically, the differences found when comparing both numerical and experimental models are more significative than those found regarding velocity. Determination coefficient, R^2, was calculated as 0,624; 0,540 and 0,501 for 7, 22 and 50 l/s scenarios, respectively. These values, in addition to being notoriously inferior to those obtained in the analysis of the velocity fields, are also quite different between different scenarios. It was concluded that the developed model

presented some limitations in the ability to reproduce the TKE values obtained experimentally. These limitations seemed to be more obvious with the increase of the flow rate.

It was concluded that the initially used mesh of 2,0 cm edges in the coarse block and 1,0 cm edge on the refined blocks was enough to simulate the flow in the flume with the desired precision.

In a general way, the results obtained in the present work prove the utility of CFD models for engineering purposes. In this study, the model allowed to adequately characterize the velocity field in the flume. In terms of TKE distribution in the flume, the developed model presented some limitations, which can be overcome in future works.

The utility of FLOW-3D® in the study of alternative configurations should be highlighted. After properly calibrated, the initial model, based on experimental results, it was possible to characterize the flow in the presence of different types of shelters. This possibility allows a reduction of time and costs invested in experimental tests, besides making possible the characterization of the flow around geometric singularities, which can be complex in laboratory.

Increased use of CFD models and their validation in eco-hydraulics increases confidence in the use of CFD models, allowing engineering and ecology together to develop efficient protection systems of species facing the hydropeaking phenomenon.

5. BIBLIOGRAPHY

Almeida, R., Boavida, I. & Pinheiro, A., 2014. Habitat numerical modelling to assess fish shelter design under hydropeaking conditions. Em *River Flow 2014*. pp. 2315–2320.

Boavida, I. et al., 2015. Barbel habitat alterations due to hydropeaking. *Journal of Hydro-environment Research*, pp.1–11.

Charmasson, J. & Zinke, P., 2011. *Mitigation Measures Against Hydropeaking*,

Clarke, K.D. et al., 2008. Validation of the Flow Management Pathway : Effects of Altered Flow on Fish Habitat and Fishes Downstream from a Hydropower Dam. , p.118.

Flow Science, I., 2018. FLOW-3D Website. Available at: www.flow3d.com.

Harby, A. & Noack, M., 2013. *Rapid Flow Fluctuations and Impacts on Fish and the Aquatic Ecosystem*,

Heimerl, S., Krueger, Æ.F. & Wurster, H., 2008. Dimensioning of fish passage structures with perturbation boulders. , pp.197–204.

Lúcio, I., 2015. Modelação numérica do escoamento deslizante sobre turbilhões em descarregadores de cheias em degraus: aplicação a pequenas barragens de aterro.

Meile, T., 2006. Hydropeaking on Watercourses. , (October 1907), pp.28–29.

Nunes, A.F.P., 2017. *Modelação computacional do escoamento deslizante sobre turbilhões em descarregadores de cheias em degraus com paredes convergentes. Dissertação de mestrado, IST, Lisboa*.

Pereira, E.N. dos R., 2016. *livre e emulsionamento de ar . Descarregador complementar de cheias da barragem de Salamonde*. Instituto Superior Técnico.

Person, É., 2013. Impact of hydropeaking on fish and their habitat. *Communications du Laboratoire de Constructions Hydrauliques - 55*, 5812(2013), p.139.

Quaresma, A.L., Ferreira, R.M.L. & Pinheiro, A.N., 2017. Comparative analysis of particle image velocimetry and acoustic Doppler velocimetry in relation to a pool-type fishway flow. *Journal of Hydraulic Research*, 55(4), pp.582–591.

Ribi, J.-M. et al., 2010. Fish behaviour during hydropeaking in a channel equipped with a lateral shelter. *8th International Symposium on Ecohydraulics*, pp.675–682.

Ribi, J.M. et al., 2014. Attractiveness of a lateral shelter in a channel as a refuge for juvenile brown trout during hydropeaking. *Aquatic Sciences*, (Sfoe 2013).

Santos, J.M. et al., 2014. Retro fitting pool-and-weir fishways to improve passage performance of benthic fishes : Effect of boulder density and fishway discharge. , 73, pp.335–344.

Scruton, D.A. et al., 2008. A synopsis of «hydropeaking» studies on the response of juvenile Atlantic salmon to experimental flow alteration. *Hydrobiologia*, 609(1), pp.263–275.

Silva, M.R., 2013. Modelação numérica 3D de escoamentos em descarregadores de cheias com escoamento em superfície livre. Descarregador complementar de Salamonde. , p.157.

Young, P.S., Cech, J.J. & Thompson, L.C., 2011. Hydropower-related pulsed-flow impacts on stream fishes: a brief review, conceptual model, knowledge gaps, and research needs. , 21(4), pp.713–731.